Footshock-Induced Activation of the Claustrum-Entorhinal Cortical Pathway in Freely Moving Mice

Wushuang HUANG[1]*, Jing QIN[1]*, Chunqing ZHANG[2], Han QIN[3], Peng XIE[1]

** These authors contributed equally to this work.*

[1]Department of Neurology, The First Affiliated Hospital of Chongqing Medical University, Chongqing, China, NHC Key Laboratory of Diagnosis and Treatment on Brain Functional Diseases, Chongqing Medical University, Chongqing, China, [2]Department of Neurosurgery, Xinqiao Hospital, Army Medical University, Chongqing, China, [3]Center for Neurointelligence, School of Medicine, Chongqing University, Chongqing, China

Received March 16, 2022
Accepted July 12, 2022
Epub Ahead of Print August 31, 2022

Summary

Footshock is frequently used as an unconditioned stimulus in fear conditioning behavior studies. The medial entorhinal cortex (MEC) contributes to fear learning and receives neuronal inputs from the claustrum. However, whether footshocks can induce a neuronal response in claustrum-MEC (CLA-MEC) projection remains unknown. Here, we combined fiber-based Ca^{2+} recordings with a retrograde AAV labeling method to investigate neuronal responses of MEC-projecting claustral neurons to footshock stimulation in freely moving mice. We achieved successful Ca^{2+} recordings in both anesthetized and freely exploring mice. We found that footshock stimulation reliably induced neuronal responses to MEC-projecting claustral neurons. Therefore, the footshock-induced response detected in the CLA-MEC projection suggests its potential role in fear processing.

Key words

Claustrum •·Fear·• Footshock •·Fiber photometry •·GCaMP

Corresponding authors

P. Xie, Department of Neurology, The First Affiliated Hospital of Chongqing Medical University, Chongqing, 400016, China; NHC Key Laboratory of Diagnosis and Treatment on Brain Functional Diseases, Chongqing Medical University, Chongqing, 400016, China. E-mail: xiepeng@cqmu.edu.cn and H. Qin, Center for Neurointelligence, School of Medicine, Chongqing University, Chongqing, 400044, China. E-mail: qinhan@cqu.edu.cn

Introduction

Fear, which can elicit defensive behaviors to avoid or reduce harm, is an important emotion for survival [1,2]. Fear is regulated by multiple brain regions and complex neural circuits. The amygdala nuclei are essential for the acquisition and expression of fear [3,4]. Fear responses are involved in dispersed brain networks, such as the sensory cortex, the medial prefrontal cortex, the hippocampus and the entorhinal cortex [1,5]. Footshock-induced pain is frequently used as the unconditioned stimulus in fear conditioning experiment paradigms [4,6]. The claustrum, a slender region underneath the cortical area, has a neuroanatomical basis that allows it to participate in high-order functions [7,8]. The medial entorhinal cortex (MEC), which has been reported to participate in fear learning, receives neuronal projections from the claustrum [9-11]. Thus, the neuronal projection from the claustrum to the MEC (CLA-MEC) may be involved in fear processing [9]. However, whether footshock can induce any response in the CLA-MEC projection remains unknown.

Real-time monitoring approaches are needed to answer this question. Traditional electrophysiological recording provides the highest temporal resolution in neural activity recording. Combined with optogenetics, optrodes provide cell-type or projection information for recorded neurons [11-14]. However, the application of

this technique is limited by a low recording efficiency. Two-photon microscopy provides a high recording efficiency but is restricted to cortical areas in anesthetized or head-fixed animals [15,16]. Fiber photometry combined with genetically encoded Ca^{2+} indicators provides a simple but efficient method for projection-specific recording in freely moving animals [17,18]. Recent studies have developed recording methods in the claustrum in freely moving mice [19,20]. However, the real-time recording of a specific CLA-MEC projection under specific behavioral tasks is still lacking.

Here, we utilized fiber-based Ca^{2+} recording to investigate the possible role of the CLA-MEC projection in footshock-induced neural responses. We observed a stable labeling of MEC projection neurons in the claustrum by local injection of retrograde AAV carrying the Ca^{2+} indicator GCaMP6m gene into the MEC. The method was then validated by Ca^{2+} recording in anesthetized and freely moving mice. Moreover, we performed Ca^{2+} recording of MEC projection neurons in the claustrum with the application of footshock stimuli in freely moving mice. Robust neuronal responses of these neurons to footshock stimuli were observed, suggesting a possible role of CLA-MEC projection in fear-related information processing.

Methods

Animals

Eleven adult male C57BL/6J mice (aged between 8-12 weeks) were used for all described studies. Mice were housed in groups under 12-hour light/dark cycle conditions, with *ad libitum* access to food and water. All experiments were performed according to institutional animal welfare guidelines and were approved by the Third Military Medical University Animal Care and Use Committee.

Optical setup

A custom-built fiber photometry system was used to record Ca^{2+} activity. Excitation light with a wavelength of 488 nm (Coherent, OBIS 488 LX-50 mW) was delivered to tissue by an optical fiber with a diameter of 200 μm (Doric Lenses, MFP_200/230/900-0.48). The optical fiber was glued into a short metal cannula (ID 0.51 mm, OD 0.82 mm, length 18 mm) with a fiber tip extending ~3.5 mm out of the cannula. Emission fluorescence was detected with an avalanche photodiode (Hamamatsu Photonic, Si APD, S2382). Data acquisition was controlled by user-customized software on the LabVIEW platform (LabVIEW 2014, National Instruments).

Virus injection

The mice were anesthetized with 1.5 % isoflurane in pure oxygen for 3-5 min. mice were then moved onto a stereotactic apparatus with a heating pad that maintained a temperature of approximately 37 °C during the entire surgery, and anesthesia was maintained by continuous delivery of isoflurane. The hair at the top of the head was shaved, and an 8-10-mm-long incision was made along the midline. Then, one small craniotomy (0.5×0.5 mm) above the MEC (AP: -4.9 mm, ML: 3.5 mm) was made. A glass micropipette with a tip diameter of ~10 μm was inserted down to a depth of 2.5 mm (from the dura) to infuse the virus. Approximately 300 nl of retroAAV-GCaMP6m viral solution was gradually injected while the micropipette was slowly lifted to a depth of 1.5 mm. Each injection took 5-10 min. The micropipette was kept in place for 5 min before being slowly withdrawn. After virus injection, the scalp wound was closed with surgical sutures, and each mouse was kept in a warm plate. Mice were then returned to their home cage for recovery. Meloxicam oral suspension (Metacam) was provided in drinking water for three days after surgery.

Fiber recording in anesthetized mice

Recording experiments were conducted approximately one month after virus injection. The preprocessed fiber probe was slowly inserted through another craniotomy above the claustrum (AP: 1.1 mm, ML: 2.5 mm) to a depth of ~2.7 mm. After the fiber probe was secured to the skull by UV-curing hardening dental cement (Tetric EvoCeram, 595953WW), the concentration of isoflurane was increased to 1.8 %. Following an adaptation period of 10 min, Ca^{2+} recordings were performed for 10 min at each anesthesia level, and the initial 3 min of each level was excluded for data analysis. The concentrations of isoflurane were 1.8 %, 1.5 %, 1.2 %, and 0.8 %.

Fiber recording in freely moving mice

The cannula was fixed to the mouse skull with dental cement after recording data from the mice in an anesthetized state, and then the mice were returned to their home cages for recovery. Meloxicam oral suspension (Metacam) was provided in drinking water

immediately after surgery for three days. Freely moving mice were placed into an opaque plastic rectangular box (30×17 cm) for 30 min. Ten sound stimulation trials (8944 Hz pure tone, 1 s, 70 dB sound pressure level, 3 min inter-sound interval) were played for mice. Subsequently, mice were moved to an electric shock box (50×50 cm) for 10 footshock trials (1 s, 0.6 mA, 3 min inter-shock interval). In the meantime, a camera was set above the recording box to monitor the behaviors of the mice. Ca^{2+} signals and mouse behaviors were recorded simultaneously. Event markers were used to synchronize the Ca^{2+} signals and behavior videos.

Histology and imaging

All experimental mice were perfused after recording to confirm the virus expression areas and fiber positions. Mice were perfused with phosphate-buffered saline (PBS) for ~5 min and then with 4 % paraformaldehyde for 15-20 min to ensure complete tissue fixation. Brain samples were collected and placed in 4 % paraformaldehyde overnight at 4 °C. Brain tissue was sectioned into 50-μm-thick slices with a freezing microtome and then stained with 4',6-diamidino-2-phenylindole (DAPI). Fluorescent images were collected with a fluorescent microscope using a 2.5× or 4× objective.

Data analysis and statistics

The Ca^{2+} data were acquired at a sampling rate of 2000 Hz and analyzed as previously described [18,21,22]. A Savitzky-Golay finite-impulse smoothing filter (50 side points and 3 polynomial orders) was first applied to the data. Then, the relative fluorescence change was calculated by $\Delta f/f = (f - f_{baseline})/f_{baseline}$, where $f_{baseline}$ was the baseline fluorescent intensity. A transient was identified as a Ca^{2+} event if the amplitude was three times larger than the standard deviation of the baseline segment.

Nonparametric and 1-way ANOVA with *post hoc* Tukey's multiple comparisons tests in MATLAB (MATLAB 2016b, MathWorks) were used for comparison. All summarized data were from individual mice and plotted as the mean ± SEM.

Results

Specific labeling of claustral neurons that project to the MEC by GCaMP6m

We used the fiber photometry system [18,21,22] to monitor the population Ca^{2+} activity of claustral neurons that project to the MEC (CLA^{MEC}-projecting neurons, Fig. 1a). We expressed the genetically encoded Ca^{2+} sensor GCaMP6m [23] specifically in CLA^{MEC}-projecting neurons by injecting retroAAV-syn-GCaMP6m [24] into the MEC (Fig. 1b, c). Then, an optical fiber was implanted above the claustrum to record the Ca^{2+} activity from CLA^{MEC}-projecting neurons (Fig. 1b, d). The expression of GCaMP6m was verified and was restricted in the MEC by *post hoc* histology (Fig. 1e). Robust expression of GCaMP6m in the claustrum was also confirmed (Fig. 1f).

Population Ca^{2+} recordings of MEC-projecting claustral neurons in anesthetized mice

Next, we determined whether the Ca^{2+} signals in the claustrum could be recorded by optical fibers with our labeling method. The Ca^{2+} signals of CLA^{MEC}-projecting neurons were recorded under different anesthesia levels by isoflurane. Figure 1g shows examples of Ca^{2+} signals from CLA^{MEC}-projecting neurons at decreasing anesthesia levels (1.8 %, 1.5 %, 1.2 %, and 0.8 %). We observed slow oscillation-associated population Ca^{2+} events, similar to the observations that have been previously described in the cortex [21,25-27], in CLA^{MEC}-projecting neurons. The amplitude and frequency of the Ca^{2+} events changed with different anesthesia levels. The amplitude (Δf/f) decreased from 0.13±0.05 to 0.05±0.01 when the isoflurane concentration decreased from 1.8 % to 0.8 % (Fig. 1h, repeated measures 1-way ANOVA with Tukey's multiple comparisons test, F=16.37, 1.8 % vs. 0.8 %, P=0.006; 1.5 % vs. 0.8 %, P=0.0002; 1.2 % vs. 0.8 %, P=0.007). Meanwhile, the frequency increased from 0.36±0.05 Hz to 3.29±0.35 Hz under these conditions (Fig. 1i, repeated measures 1-way ANOVA with Tukey's multiple comparisons test, F=37.27, 1.8 % vs. 1.5 %, P=0.03; 1.8 % vs. 1.2 %, P=0.00004; 1.8 % vs. 0.8 %, P=0.00003, 1.5 % vs. 1.2 %, P=0.004; 1.5 % vs. 0.8 %, P=0.002). Thus, the retrograde labeling method can be combined with fiber photometry for real-time neural activity recording of CLA^{MEC}-projecting neurons.

Population Ca^{2+} response in MEC-projecting claustral neurons induced by footshock in freely behaving mice

To investigate the response induced by footshock in freely moving mice, we conducted optical fiber recordings of CLA^{MEC}-projecting neurons together with behavioral video surveillance. We performed the recordings at least 5 days after fiber implantation. Mice

were placed in a white rectangular box for free exploration, with an infrared camera placed above them to monitor their behavior (Fig. 2a). Figure 2b shows a 200-s recording of Ca^{2+} signals (black trace) synchronized with body movements (gray trace). Mouse locations during the corresponding recording period were automatically tracked and are plotted in Figure 2c. According to both the example in Figure 2b and statistical analysis in Figure 2d, we found significantly higher Ca^{2+} signals during locomotion than during grooming behavior (Fig. 2d, two-sided Wilcoxon rank-sum test, z=6.3, P=2.88e-10).

We next performed fiber recordings of CLA^{MEC}-projecting neurons during the application of sound or footshock in freely moving mice (Fig. 2e). We found that sound stimulation could not induce any Ca^{2+} signal (four example trials from one mouse in Fig. 2f, left; summary of 19 trials from 3 mice in Fig. 2g), while footshock stimulation induced clear and stable responses from CLA^{MEC}-projecting neurons (four example trials from one mouse in Fig. 2f, right; summary of 21 trials from 3 mice in Fig. 2h). The onset latency of these footshock-induced Ca^{2+} responses was 48.3±4.8 ms (21 trials from 3 mice). The peak amplitude (Δf/f) of footshock-induced Ca^{2+} responses was significantly larger than that of sound stimulation (Fig. 2i, two-sided Wilcoxon rank-sum test, z=5.3, P=1.28e-7).

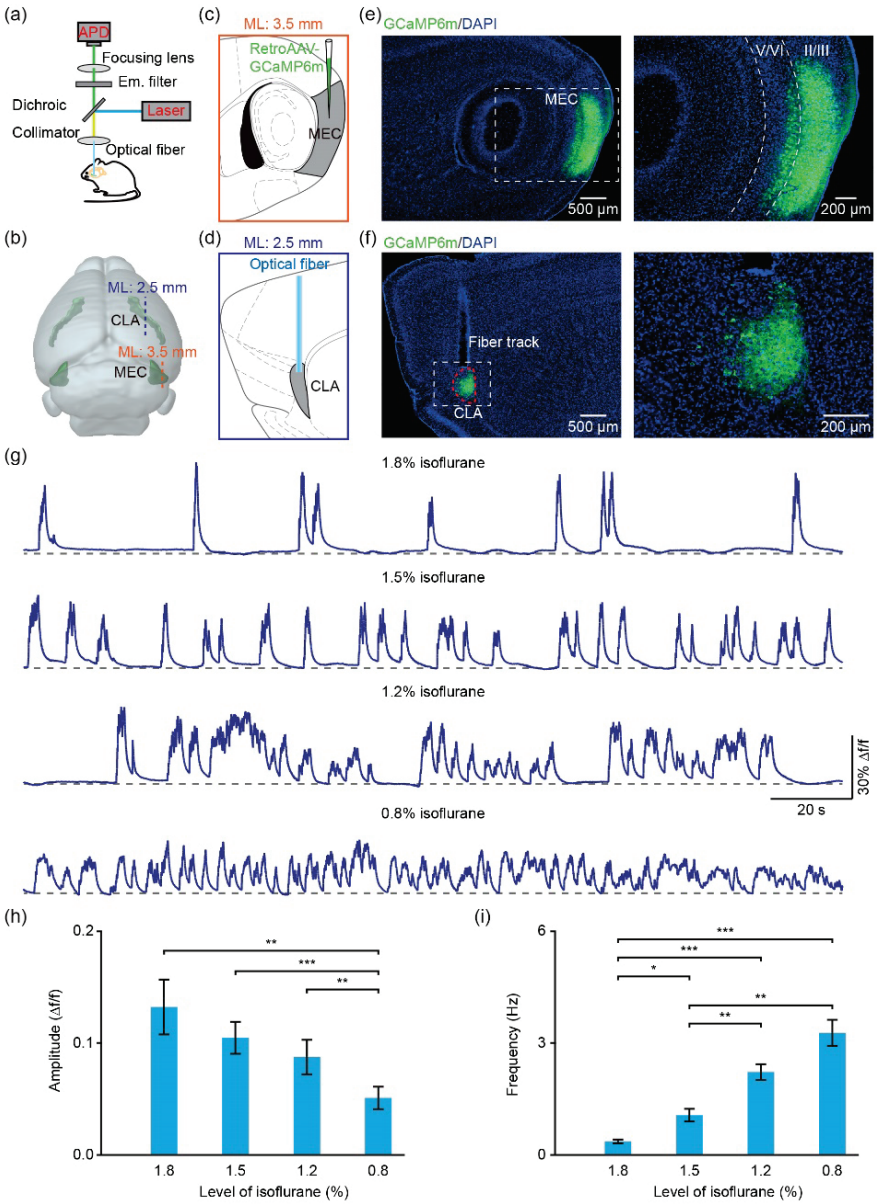

Fig. 1. Population Ca^{2+} recordings of CLA^{MEC}-projecting neurons in anesthetized mice with GCaMP6m. (**a**) Schematic of the fiber photometry setup. (**b-d**) Experimental design of retroAAV-GCaMP6m injection in the MEC (**c**) and fiber implantation in the claustrum (**d**); ML: mediolateral, CLA: claustrum; MEC: medial entorhinal cortex. (**e**) *Post hoc* histological images showing the expression of GCaMP6m in the MEC. (**f**) *Post hoc* histological confirmation of GCaMP6m expression and optical fiber position in the claustrum. (**g**) Examples showing the population Ca^{2+} signals of CLA^{MEC}-projecting neurons at different anesthesia levels. (**h**) Amplitude of Ca^{2+} events of CLA^{MEC}-projecting neurons at different anesthesia levels (n=11 mice; repeated measures 1-way ANOVA with Tukey's multiple comparisons test, ** P<0.01, *** P<0.001). (**i**) Frequency of Ca^{2+} events of CLA^{MEC}-projecting neurons at different anesthesia levels (n=11 mice; repeated measures 1-way ANOVA with Tukey's multiple comparisons test, * P<0.05, ** P<0.01, *** P<0.001).

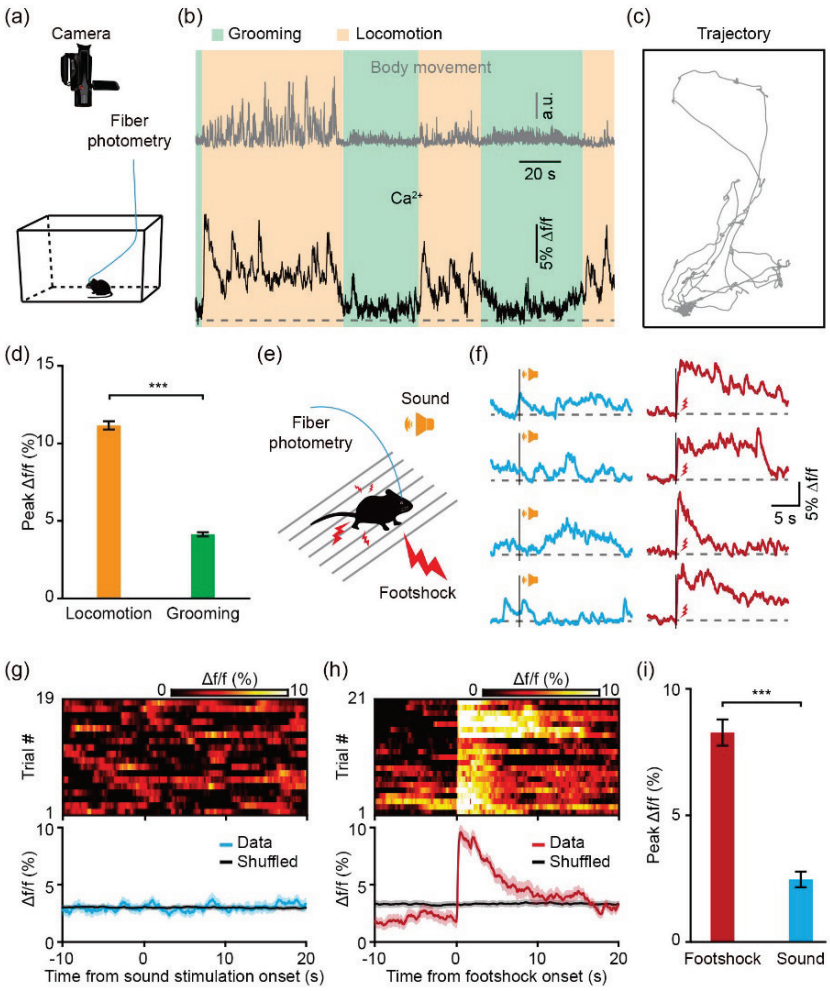

Fig. 2. Population Ca^{2+} transients of CLA^{MEC}-projecting neurons induced by footshock stimulation in freely moving mice. (**a**) Diagram of the recording setup in freely moving mice. (**b**) Example showing the relative body movements (gray trace) and the Ca^{2+} transients recorded in CLA^{MEC}-projecting neurons (black trace) in a freely moving mouse; green shaded areas: grooming; yellow shaded areas: locomotion. (**c**) The corres-ponding locomotion trajectory of the recording period in b. (**d**) Summary of peak Δf/f during locomotion or grooming (locomotion: n=31 trials from 3 mice; grooming: n=24 trials from 3 mice, two-sided Wilcoxon rank-sum test, *** P<0.001). (**e**) Schematic diagram of Ca^{2+} recording with footshock or sound stimulation. (**f**) Representative Ca^{2+} signals induced after sound (blue) or footshock (red) in CLA^{MEC}-projecting neurons from one mouse. (**g, h**) Color-coded intensities (top) and average trace (bottom) of Ca^{2+} signals aligned to sound (**g**, 19 trials from 3 mice) or footshock (**h**, 21 trials from 3 mice) stimulation. The black trace is the shuffled data, and shaded areas represent S.E.M. (**i**) Summary of peak Δf/f during sound and footshock stimulation (sound: n=19 trials from 3 mice, footshock: n=21 trials from 3 mice, two-sided Wilcoxon rank-sum test, z=5.1, *** P<0.001).

Discussion

In this study, we utilized fiber photometry to investigate the neural responses in CLA-MEC projection to footshock stimulation. We used a retrograde AAV carrying the genetically encoded Ca^{2+} indicator GCaMP6m to specifically label MEC-projecting neurons in the claustrum. To test the effectiveness of the retrograde labeling, we first performed Ca^{2+} recording in the anesthetized state by implantation of an optical fiber probe in the claustrum of retroAAV-GCaMP6m-injected mice. We found that the amplitude of the population Ca^{2+} events decreased with decreasing isoflurane concentration. In contrast, the frequency increased in this process. Then, we demonstrated Ca^{2+} recordings of CLA^{MEC}-projecting neurons in freely moving mice. Stable neuronal responses induced after footshock but not sound stimulation were detected in the CLA^{MEC}-projecting neurons. These Ca^{2+} responses after footshock could result from locomotion, pain sensation or startle reflex caused by footshock [28]. Future work is needed to differentiate these possibilities.

The claustrum has been hypothesized to be involved in higher-order processes, depending on its dense connection to and from the associative cortex [9,10,29,30]. Moreover, it has been suggested to participate in multiple brain functions, such as sensory information integration, attention and consciousness [29-32]. The projection from the claustrum to MEC has been less studied. Kitanishi *et al.* reported that CLA-MEC projection was activated by novel context and modulated contextual memory [9]. However, the real-time activity pattern of CLA-MEC projection has not been clearly investigated. Here, we showed that a fiber-based recording method combined with retrograde AAV labeling can achieve real-time recording of specific projections in freely behaving mice, which will aid our understanding of the function of specific neural projections.

Overall, we demonstrated that fiber-based Ca^{2+} recording combined with retrograde AAV labeling is ideal for real-time monitoring of CLA-MEC projection in freely moving mice. With this approach, we found

a stable and reliable response of CLA^{MEC}-projecting neurons induced by footshock stimulation. These findings may lead to a clearer understanding of neural circuits in fear learning and pain.

Conflict of Interest

There is no conflict of interest.

Acknowledgements

The authors are grateful to Ms. Jia Lou for help in composing and editing the layout of the figures. This work was supported by grants from the National Natural Science Foundation of China (82171463) to CZ and Fundamental Research Funds for the Central Universities (2022CDJXY-024) to HQ.

References

1. Tovote P, Fadok JP, Lüthi A. Neuronal circuits for fear and anxiety. Nat Rev Neurosci 2015;16:317-331. https://doi.org/10.1038/nrn3945
2. Garcia R. Neurobiology of fear and specific phobias. Learn Mem 2017;24:462-471. https://doi.org/10.1101/lm.044115.116
3. LeDoux JE. Emotion circuits in the brain. Annu Rev Neurosci 2000;23:155-184. https://doi.org/10.1146/annurev.neuro.23.1.155
4. LeDoux J. The amygdala. Curr Biol 2007;17:R868-R874. https://doi.org/10.1016/j.cub.2007.08.005
5. Wahlstrom KL, Huff ML, Emmons EB, Freeman JH, Narayanan NS, McIntyre CK, LaLumiere RT. Basolateral amygdala inputs to the medial entorhinal cortex selectively modulate the consolidation of spatial and contextual learning. J Neurosci 2018;38:2698-2712. https://doi.org/10.1523/JNEUROSCI.2848-17.2018
6. Phillips RG, LeDoux JE. Differential contribution of amygdala and hippocampus to cued and contextual fear conditioning. Behav Neurosci 1992;106:274-285. https://doi.org/10.1037/0735-7044.106.2.274
7. Jackson J, Smith JB, Lee AK. The anatomy and physiology of claustrum-cortex interactions. Annu Rev Neurosci 2020;43:231-247. https://doi.org/10.1146/annurev-neuro-092519-101637
8. Smith JB, Lee AK, Jackson J. The claustrum. Curr Biol 2020;30:R1401-R1406. https://doi.org/10.1016/j.cub.2020.09.069
9. Kitanishi T, Matsuo N. Organization of the claustrum-to-entorhinal cortical connection in mice. J Neurosci 2017;37:269-280. https://doi.org/10.1523/JNEUROSCI.1360-16.2016
10. Zingg B, Dong H-W, Tao HW, Zhang LI. Input-output organization of the mouse claustrum. J Comp Neurol 2018;526:2428-2443. https://doi.org/10.1002/cne.24502
11. Narikiyo K, Mizuguchi R, Ajima A, Shiozaki M, Hamanaka H, Johansen JP, Mori K, Yoshihara Y. The claustrum coordinates cortical slow-wave activity. Nat Neurosci 2020;23:741-753. https://doi.org/10.1038/s41593-020-0625-7
12. Anikeeva P, Andalman AS, Witten I, Warden M, Goshen I, Grosenick L, Gunaydin LA, Frank LM, Deisseroth K. Optetrode: a multichannel readout for optogenetic control in freely moving mice. Nat Neurosci 2011;15:163-170. https://doi.org/10.1038/nn.2992
13. Stark E, Koos T, Buzsaki G. Diode probes for spatiotemporal optical control of multiple neurons in freely moving animals. J Neurophysiol 2012;108:349-363. https://doi.org/10.1152/jn.00153.2012
14. Chevée M, Finkel EA, Kim SJ, O'Connor DH, Brown SP. Neural activity in the mouse claustrum in a cross-modal sensory selection task. Neuron 2022;110:486-501.e487. https://doi.org/10.1016/j.neuron.2021.11.013
15. Denk W, Strickler JH, Webb WW. Two-photon laser scanning fluorescence microscopy. Science 1990;248:73-76. https://doi.org/10.1126/science.2321027
16. Yuste R, Denk W. Dendritic spines as basic functional units of neuronal integration. Nature 1995;375:682-684. https://doi.org/10.1038/375682a0
17. Adelsberger H, Garaschuk O, Konnerth A. Cortical calcium waves in resting newborn mice. Nat Neurosci 2005;8:988-990. https://doi.org/10.1038/nn1502
18. Qin H, Fu L, Hu B, Liao X, Lu J, He W, Liang S, ET AL. A visual-cue-dependent memory circuit for place navigation. Neuron 2018;99:47-55.e44. https://doi.org/10.1016/j.neuron.2018.05.021

19. White MG, Panicker M, Mu C, Carter AM, Roberts BM, Dharmasri PA, Mathur BN. Anterior cingulate cortex input to the claustrum is required for top-down action control. Cell Rep 2018;22:84-95. https://doi.org/10.1016/j.celrep.2017.12.023
20. White MG, Mu C, Qadir H, Madden MB, Zeng H, Mathur BN. The mouse claustrum is required for optimal behavioral performance under high cognitive demand. Biol Psychiatry 2020;88:719-726. https://doi.org/10.1016/j.biopsych.2020.03.020
21. Zhang Q, Yao J, Guang Y, Liang S, Guan J, Qin H, Liao X, ET AL. Locomotion-related population cortical Ca(2+) transients in freely behaving mice. Front Neural Circuits 2017;11:24. https://doi.org/10.3389/fncir.2017.00024
22. Qin H, Lu J, Jin W, Chen X, Fu L. Multichannel fiber photometry for mapping axonal terminal activity in a restricted brain region in freely moving mice. Neurophotonics 2019;6:035011. https://doi.org/10.1117/1.NPh.6.3.035011
23. Chen TW, Wardill TJ, Sun Y, Pulver SR, Renninger SL, Baohan A, Schreiter ER, ET AL. Ultrasensitive fluorescent proteins for imaging neuronal activity. Nature 2013;499:295-300. https://doi.org/10.1038/nature12354
24. Tervo DG, Hwang BY, Viswanathan S, Gaj T, Lavzin M, Ritola KD, Lindo S, ET AL. A designer aav variant permits efficient retrograde access to projection neurons. Neuron 2016;92:372-382. https://doi.org/10.1016/j.neuron.2016.09.021
25. Luczak A, Bartho P, Marguet SL, Buzsaki G, Harris KD. Sequential structure of neocortical spontaneous activity in vivo. Proc Natl Acad Sci U S A 2007;104:347-352. https://doi.org/10.1073/pnas.0605643104
26. Stroh A, Adelsberger H, Groh A, Ruhlmann C, Fischer S, Schierloh A, Deisseroth K, Konnerth A. Making waves: initiation and propagation of corticothalamic Ca2+ waves in vivo. Neuron 2013;77:1136-1150. https://doi.org/10.1016/j.neuron.2013.01.031
27. Adelsberger H, Grienberger C, Stroh A, Konnerth A. In vivo calcium recordings and channelrhodopsin-2 activation through an optical fiber. Cold Spring Harb Protoc 2014;2014:pdb prot084145. https://doi.org/10.1101/pdb.prot084145
28. Zhang K, Förster R, He W, Liao X, Li J, Yang C, Qin H, ET AL. Fear learning induces α7-nicotinic acetylcholine receptor-mediated astrocytic responsiveness that is required for memory persistence. Nat Neurosci 2021;24:1686-1698. https://doi.org/10.1038/s41593-021-00949-8
29. Liu J, Wu R, Johnson B, Vu J, Bass C, Li J-X. The claustrum-prefrontal cortex pathway regulates impulsive-like behavior. J Neurosci 2019;39:10071-10080. https://doi.org/10.1523/JNEUROSCI.1005-19.2019
30. Terem A, Gonzales BJ, Peretz-Rivlin N, Ashwal-Fluss R, Bleistein N, Del Mar Reus-Garcia M, Mukherjee D, Groysman M, Citri A. Claustral neurons projecting to frontal cortex mediate contextual association of reward. Curr Biol 2020;30:3522-3532.e3526. https://doi.org/10.1016/j.cub.2020.06.064
31. Atlan G, Terem A, Peretz-Rivlin N, Sehrawat K, Gonzales BJ, Pozner G, Tasaka G-I, ET AL. The claustrum supports resilience to distraction. Curr Biol 2018;28:2752-2762.e2757. https://doi.org/10.1016/j.cub.2018.06.068
32. Jackson J, Karnani MM, Zemelman BV, Burdakov D, Lee AK. Inhibitory control of prefrontal cortex by the claustrum. Neuron 2018;99:1029-1039.e1024. https://doi.org/10.1016/j.neuron.2018.07.031